Authors:

Name: Jiri Silha (author for correspondence)
Address: Astronomical Institute, University of Bern, CH-3012 Bern, Switzerland
Email: jiri.silha@aiub.unibe.ch

Name: Thomas Schildknecht
Address: Astronomical Institute, University of Bern, CH-3012 Bern, Switzerland,
Email: thomas.schildknecht@aiub.unibe.ch

Name: Andreas Hinze
Address: DLR, Münchner Strasse 20, 82234 Wessling, Germany
Email: andreas.hinze@dlr.de

Name: Tim Flohrer
Address: Space Debris Office, ESA/ESOC, Robert-Bosch-Str. 5, 64293 Darmstadt, Germany
Email: tim.flohrer@esa.int

Name: Alessandro Vananti
Address: Astronomical Institute, University of Bern, CH-3012 Bern, Switzerland
Email: alessandro.vananti@aiub.unibe.ch

*Corresponding author: Tel: +41-316318602
Email address: jiri.silha@aiub.unibe.ch

An Optical Survey for Space Debris on Highly Eccentric and Inclined MEO Orbits

J. Silha[1,4*], T. Schildknecht[1], A. Hinze[2], T. Flohrer[3], A. Vananti[1]

[1]Astronomical Institute, University of Bern, CH-3012 Bern, Switzerland
[2]DLR, Münchner Strasse 20, 82234 Wessling, Germany
[3]Space Debris Office, ESA/ESOC, Robert-Bosch-Str. 5, 64293 Darmstadt, Germany
[4]Faculty of Mathematics, Physics and Informatics, Comenius University, Mlynská dolina, 84248 Bratislava, Slovakia

[*] Author for correspondence: E-mail: jiri.silha@aiub.unibe.ch

Abstract

Optical surveys for space debris in high-altitude orbits have been conducted since more than ten years. Originally these efforts concentrated mainly on the geostationary region (GEO). Corresponding observation strategies, processing techniques and cataloguing approaches have been developed and successfully applied. The ESA GEO surveys, e.g., resulted in the detection of a significant population of small-size debris and later in the discovery of high area-to-mass ratio objects in GEO-like orbits. Comparably less experience (both, in terms of practical observation and strategy definition) is available for eccentric orbits that (at least partly) are in the MEO region, in particular for the Molniya-type orbits.

Different survey and follow-up strategies for searching space debris objects in highly-eccentric MEO orbits, and to acquire orbits which are sufficiently accurate to catalogue such objects and to maintain their orbits over longer time spans were developed. Simulations were performed to compare the performance of different survey and cataloguing strategies. Eventually, optical observations were conducted in the framework of an ESA study using ESA's Space Debris Telescope (ESASDT) the 1-m Zeiss telescope located at the Optical Ground Station (OGS) at the Teide Observatory at Tenerife, Spain.

Thirteen nights of surveys of Molniya-type orbits were performed between January and August 2013. Eventually 255 surveys were performed during these thirteen nights corresponding to about 47 hours of observations. In total 30 uncorrelated faint objects were discovered. On average one uncorrelated object was found every 100 minutes of observations. Some of these objects show a considerable brightness variation and have a high area-to-mass ratio as determined in the orbit estimation process.

Key words: space debris, optical surveys, Molniya orbits, space debris environment modeling

INTRODUCTION

Space debris population in the low Earth orbit (LEO) region, which is defined as a region up to 2000 kilometers altitude, has been extensively studied during the last decades and reasonable models like ESA MASTER model (Wiedemann et al., 2011, Flegel et al., 2011) and NASA ORDEM model (Krisko at al., 2015, Xu et al., 2009) which are covering all size ranges were produced. Recognizing the paramount importance of protecting the geostationary orbit (GEO) region from contaminating space debris, the European Space Agency (ESA) initiated in 1999 an optical search for fragments in the GEO and GTO (geosynchronous

transfer orbit) to improve the knowledge about their debris population and to understand the future evolution of these objects (Schildknecht et al., 2004, 2005). For completeness we should also mention that similar GEO surveys have been performed also by other teams worldwide such as Abercromby et al. (2009) or Molotov et al. (2008).

The space debris environment in the medium Earth orbit (MEO) region has not been systematically investigated so far and is thus largely unknown. Recently, an extension of the ongoing space debris surveys to new orbital regions, in particular to the increasingly populated MEO region was undertaken (Schildknecht et al., 2012). In the latter study the work focused more on circular MEO orbits, including GPS and GLONASS constellations. The observation of highly-eccentric MEO orbits presented in this paper is a further extension of this previous study. These eccentric and high elliptical orbits include in particular Molniya and Tundra orbits. Molniya orbits have an inclination of around 63.4°, mostly an argument of perigee of about -90° and a revolution period of one half of a sidereal day. With an eccentricity around 0.7 and an apogee altitude around 40,000 km, the orbit is conceived such that a spacecraft would spend a considerable period of time around apogee over the northern hemisphere. Some of the Molniya population has orbits with an argument of perigee around 90°. Objects on these orbits spend most of their time above the southern hemisphere. The 63.4° inclination is chosen to minimize the secular perturbation of the argument of perigee caused by the Earth's oblateness (Beutler, 2005). In comparison Tundra orbits have the same inclination comparing to Molniya but an orbital period of one sidereal day. The primary task of spacecraft on Molniya type of orbits is, in most cases, to enable military and commercial communication.

In our paper we present the catalogued Molniya population with its dynamical characteristics. Furthermore, this population was used to develop the observation survey strategy to search for new uncatalogued objects. Finally, the paper presents the results from thirteen nights of surveys performed in 2013 with ESADT telescope which is part of the Optical Ground Station (OGS) situated in Tenerife, Canary Islands, Spain.

MOLNIYA POPULATION

In order to select the objects of interest during the development of a survey, we defined within this paper Molniya objects as objects with orbital elements fulfilling following criteria. For orbital inclination the boundaries were assumed at 60° and 67°, for eccentricity at 0.5 and 0.8 and for semi-major axis at 20,000 and 30,000 km. The semi-major axis interval corresponds to a mean motion between 3.0 and 1.7 revolutions per day. We did not set any limits in right ascension of the ascending node (Ω) and in the argument of the perigee (ω).

Catalogue population

In the publicly available USSTRATCOM catalogue (www.space-track.org), a total of 171 unclassified Molniya objects as of January 2012 (hereafter referred to as the selected TLE population) were found. This selected TLE population includes Molniya satellites (41), Meridian satellites (4), Oko satellites, rocket body or upper stages (73), as well as some other types of debris (53). Fig 1. shows distributions of orbital elements for the selected TLE population. The nodes are distributed over the whole range of right ascension with a concentration between 0° and 210° and the inclinations are concentrated around the nominal value of 63.4° (the so-called critical inclination) (Beutler, 2005). Based on the distribution of the eccentricity it was possible to separate a subgroup from the selected Molniya population with $e < 0.65$. This subgroup consists of 35 objects including rocket bodies (10), debris (20) and Russian Oko satellites (5) with an eccentricity of less than 0.65.

The relations between the orbital elements of the selected TLE population are shown in Fig. 2, where objects with an eccentricity of less than 0.65 are given by the crosses. Objects with a perigee less than 180° and therefore with an apogee above the southern hemisphere are given by the empty squares. The rest of the population is given by the filled circles. For a ground-based sensor, such objects in highly-eccentric orbits and with a mean motion of about two revolutions per day, show at the point of their perigees relatively high angular velocities with respect to the stars. Therefore it would be difficult to observe objects around this position. From all selected TLE objects, 55 objects have an argument of perigee between 0° and 180°, which means that these perigees are located above the northern hemisphere.

Fig. 3 (left) shows apparent passes of the selected TLE population in the right ascension and declination (RA/DE) system as seen from the OGS during one night in January 2012. There is a region with an enhanced apparent density in the declination stripe between 55° and 65°. In this culmination region most of the objects, namely the objects whose orbits have an argument of perigee around 270° (marked in Fig. 2 as black dots and crosses) reach their apogee.

Since implementing an efficient detection strategy requires the optimization of the tracking rates and the integration time, we prefer regions where the changes in apparent velocity are small. Fig. 3 (right) shows the topocentric angular velocity in the RA/DE coordinate system as a function of declination as seen from the OGS. The minimal angular velocity is around 5.5 arc-sec/s for objects with a declination between 60° and 70°. Objects with a perigee around 90° reach their minimal angular velocity at a declination between -30° and -40°. Unfortunately, these are the regions that are barely visible from the OGS location.

Evolution of orbital elements

The gravitational and non-gravitational forces are constantly affecting dynamics of every object placed on the geocentric orbit. Consequently, these forces cause that the object orbital elements might change significantly over the time. In order to find out on which types of orbit former Molniya objects could be found today and to better optimize our survey strategy, we took the selected TLE population and simulated the evolution of the orbital elements for twenty years into the future. For this propagation a full force model was used including the gravitational attraction of the Sun and the Moon, the Earth's gravitational potential coefficients up to terms of degree and order 12, the perturbations due to the Earth tides, the corrections due to the general relativity, and a simple model for the direct radiation pressure. An area-to-mass ratio (*AMR*) of 0.009 m^2/kg for both, the air drag and radiation pressure, was used. We set the value for the drag coefficient to 2.0 for all objects, which means a spherical shape was assumed for them **(**Beutler, 2005**)**. For the solar radiation coefficient, which depends on the reflectivity properties of the object, a value of 2.0 was set during the integration.

Fig. 4 shows the evolution of orbital elements over 20 years. Objects with an eccentricity of less than 0.65 are given in gray. The daily drift of nodes for the selected TLE population ranges from -31 to -73 °/year, with a median value of -45°/year, which corresponds to a drift of -0.08 to -0.2°/day and a median of -0.12°/day. Most of the objects keep their eccentricity and inclination stable over the simulated time interval, whereas objects with an initial eccentricity of less than 0.65 and an inclination of more than 65° show a variation of the inclination and argument of perigee. An inclination of more than 63.4° causes a negative drift of the perigee. Therefore the arguments of perigee of these objects drift to lower values during the simulated 20 years. For this population the eccentricity is slightly increasing. Finally, some of the TLE objects reentered the Earth atmosphere during the simulated 20 years. These objects have the incomplete evolution in orbital elements during the investigated period.

Fig. 5 gives the comparison between orbital elements of the selected TLE population (black) and its 20 years prediction (gray). Fig. 5 shows that there are no significant differences between both distributions. Because of the drift of the RAAN, the maxima have been shifted to different values, as expected. Relative frequencies are given, as more than 40 % of the objects were lost because they re-entered the atmosphere within the 20 years.

Objects with an inclination around 63.4° show no significant changes in inclination after 20 years, which is in agreement with the theory. If the initial inclination is, however, higher than 65°, the distribution of the inclination after the investigated time span has expanded up to a maximum of 72°. Based on the fact that the oldest Molniya objects have been in orbit for more than 30 years, one could expect that some of the objects would reach even higher inclinations. However, the analysis of the TLE population (January 2012) showed that so far no objects with an inclination higher than 72° are present in the TLE population, which means that the TLE Molniya population is covered by this paper's limits for the eccentricity and semi-major axes. Consequently, taking into account that the oldest objects have been in orbit for about 30 years, one can expect that the current distribution roughly and sufficiently well represents the initial distribution and it can be used for the development and testing of a Molniya survey strategy.

OBSERVATION STRATEGY

During the development of the survey strategy, we investigated three different strategy options by using different architectures and logic during the night. We investigated for all three options their coverage efficiency by assuming different number of available observation nights.

Survey strategies

To investigate the coverage efficiency of the Molniya population by using different observation scenarios, a synthetic population within following limits was simulated. For the inclination the set interval was between 62° and 67°, for eccentricity between 0.5 and 0.75 and for semi-major axis between 23,000 km and 27,000 km. A uniform distribution of all orbital elements within the mentioned ranges was assumed. We set no limit for the nodes and for the arguments of perigee.

About 900 objects of this synthetic population were selected (see Fig. 6) in a way to best represent the TLE population distribution (Fig. 2) and relations between the orbital elements. This synthetic population was used to simulate the coverage with ESA's Program for Radar and Optical Observation Forecasting (PROOF) (Krag et al., 2001, Flegel et al., 2011). During the simulation every object was modeled as a sphere with a diameter of 1 m and a geometric albedo of 0.1.

We used in PROOF the FoV, exposure and gap times of the ESASDT configuration. Three similar observation strategies (see Fig. 7) have been simulated over a time span of 90 days where the total observations time was the same for each of them. A survey declination of 55° was chosen for all strategies to guarantee that from the geometrical point of view all objects would be possible to track. This is the declination where the selected TLE (Molniya) objects with lowest inclinations reach their culmination point when they are observed from the OGS. In all cases the fields were selected with the right ascension close to the opposite to the Sun to ensure best phase angle conditions. In the first strategy a single field was assumed. In the second strategy a fence of three fields has been observed whereas the field in the middle of this fence was identical with that one of the first strategy. The two additional fields were

displaced by 0.5° in right ascension. Finally, in the third strategy a fence consisting of four fields was simulated. The first field was identical with that one from the first strategy and all additional fields have been displaced +0.5° in right ascension with respect to each other.

In the first scenario 35 objects could be detected during the simulated 90 days of surveys, while in the second and third scenarios just a few more objects were detected although the covered region is larger in comparison with the first scenario. During 90 days 44 and 46 objects could be detected for these two strategies, respectively. The results of these three strategies are similar in terms of number of detected objects and even when the covered field was three time bigger only a few more objects could be found. However, such results were expected because the observation strategy was designed the way that the objects are detected close to their culmination points where they apparent motion is mostly in the right ascension. This can be seen in Fig. 3, left. Because the survey fields are shifted from each other also only in right ascension and not in declination it is often the case that the same object would be seen in adjacent fields.

Coverage simulation

Because of the small FoV of the ESASDT telescope of 0.7 deg, and the limited availability of the OGS for space debris surveys, it would be over-ambitious to cover the whole Molniya region by surveys. Therefore simulations over one year with three consecutive nights of observation per month have been performed. This number of nights was chosen, because of the limited observation time available for Molniya surveys with the ESASDT. The first observation strategy was assumed. The field was displaced by 10° in right ascension each night such that the right ascension of the field centers was always near the anti-sun direction (see Fig. 8). For the survey declination 55° were chosen. After one year of simulated surveys about 25 % of the synthetic population, whose orbital elements are plotted in Fig. 6 crossed the FoV and more than 60 % of them could be detected on at least one frame which corresponds to about 16 % of the synthetic population. Four different parameters distributions of objects which crossed the FoV (crossings) are shown in Fig. 9. Plotted are angular velocities, FoV crossing times, magnitudes and phase angles. The phase angle values varied between 25° to 90° due to the annual apparent motion of the anti-sun point on the celestial sphere.

These results are promising. By performing observations during three nights per month, only 10% of the available total sensor time is used, but a proportionally exceeding number of 16% of the total number objects could be detected.

SURVEYS PERFORMED AT ESA OPTICAL GROUND STATION

From January to August 2013 thirteen surveys dedicated to the Molniya objects were performed with the ESA Space Debris Telescope (ESASDT) at the Optical Ground Station (OGS), Observatorio del Teide, Tenerife. During one observation unit a single geocentric field was observed for 11 minutes. If a faint object was found, one or two follow-up observations were performed during the same night to ensure a save rediscovery during the next nights. The first follow-up took place 15-20 minutes after the discovery. If there was time available and the object was still above the horizon, the second follow-up was performed 45-50 minutes after the discovery. Our experience in the past showed that this approach is sufficient for ensuring successful follow-up observations of the discovered objects during next night.

All observations of the same object within a single FoV crossing constitute a so-called tracklet. The tracklet is set of observations over shorter period of time which presumably belong to the same object. If there were three or more tracklets of one object during the discovery night, an orbit was determined and inserted into an internal catalogue, and this object was scheduled for further observations with the ESASDT and AIUB's ZIMLAT telescopes during following nights.

In total, there were thirteen survey nights, namely three nights in January, February, April and July and one night in August 2013. Thirteen FoVs were surveyed, one each night, where all of them were defined by the geocentric right ascension and declination, and by assuming a geocentric distance of 41,000 km to correct for the parallax. The declination was set to 63.0°, assuming that this would be the culmination region where we could expect the lowest angular velocity for the majority of objects (see Fig. 3).

For every one of our observation units (OU) that structured a survey, thirty frames were obtained, where an individual frame was observed for 22 s, which comprises 2 s of exposure and 20 s of readout time. During the exposure a blind tracking of 5.5 arc-sec/s in the assumed direction of motion of a typical Molniya object, was applied to maximize the signal-to-noise ratio for Molniya like objects. Altogether there were 251 OUs during the first twelve nights, between 10 and 32 OUs per night. As one OU took 11 minutes to survey, a total of 7,530 frames were obtained for processing during 46.02 hours (2761 min) of observations. For the last night in August, 4 OUs were obtained, where, different to the previous units, 1 OU comprised 29 s of read-out time and 2 s of exposure. For all thirteen surveys there were 255 OUs obtained with 7,634 frames during 46.92 hours in total. All objects were correlated with the ESA DISCOS catalogue (Hernández et al., 2001).

During thirteen nights of surveys, 30 un-correlated targets (UCTs) were discovered and their full (i.e. elliptical) orbits were determined. These cases are all objects with two and more observations per discovery night. In Fig. 10 we show the surveyed fields with their geocentric right ascension (RA) and declination (DEC).

Taking into account the whole time dedicated to the surveys, there was a new object discovered on average every 100 minutes of survey. From all 30 UCTs, 25 were catalogued by AIUB, which means that these objects had three and more tracklets per discovery night and for these objects additional follow-ups in following nights were planned. For the catalogue maintenance the follow-up observations of newly discovered objects were acquired also with AIUB´s 1-m ZIMLAT telescope in Zimmerwald, Switzerland. Because of the low brightness of the objects, occasionally bad weather conditions in Zimmerwald, and the limited time to perform continuous observations with the ESASDT, only a few follow-up observations of newly discovered objects were successful. This is also the reason why the majority of the objects were lost within few days to months after their discovery. Most UCTs were observed only during the three nights of the given campaign. There were only two cases for which the follow-ups cover more than six months.

PHYSICAL AND DYNAMICAL CHARACTERISTICS OF DISCOVERED OBJECTS

The limiting magnitude for the ESASDT system is around 19^{th} – 19.7^{th} magnitude, depending on the quality of the night, by using an exposure time of 2 s without using a filter. Fig. 11 shows the distribution of magnitudes of the discovered objects. The majority of objects have magnitudes between 18^{th} to 19^{th}. The cutoff of the distribution at 19^{th} magnitude is given by the limitation of the observation system and not necessary by the object population. For a Lambertian sphere, with the Bond albedo of 0.2, observed under 60° phase angle from a

distance of 42,000 km (the maximum topocentric distance for Molniya population for OGS site), the 19th magnitude can be interpreted as a diameter of 0.2 meter. Clearly, the number of objects is increasing at fainter brightness (Fig. 11). The low number of objects with 19th magnitude is purely caused by a selection effect. Fainter objects were just too faint to be recognized and detected during surveys. Additionally, there is a strong selection effect also coming from the angular rates. The survey is most sensitive for objects with angular rates close to 5.5 arc-sec/s and the limiting magnitude is lower for objects with velocities substantially different from this value. For completeness we can add that all the 30 UCTs had apparent angular velocities below 35 arc-sec/s in time they were detected, where majority of them (21) had angular velocities below 10 arc-sec/s.

For some cases the brightness variability was very high (see example in Fig. 12), which caused that these objects have not been seen during some nights with the ZIMLAT telescope. This kind of behavior was already observed during the GEO surveys performed in the past with the ESASDT. During the Molniya surveys the estimated magnitude error varied between 0.2 - 1.6 mag depending on the brightness of the object and its rotational properties. These two effects were not distinguished.

For objects with longer arcs, i.e. longer than 29 days, it was possible to accurately determine their area-to-mass ratios (AMR). Results for twelve objects with sufficient observation arcs are plotted in Fig. 13. Five low area-to-mass objects with AMR < 0.01 m^2/kg, there were also five objects with AMR within the interval 0.01 – 1.0 m^2/kg. There were two high area-to-mass objects (HAMR) catalogued, namely E13010A and E13189B. For these objects we determined AMR ratios equal 3.59 m^2/kg and 3.74 m^2/kg, calculated from observation arcs of 235.17 days and 57.4 days, respectively.

Molniya UCTs that we could maintain in the AIUB internal catalogue showed, as expected, similar orbital elements distribution as the selected TLE population. Several types of orbital elements are plotted in Fig. 14. For the right ascension of ascending node (RAAN) (upper figure) for UCTs there are gaps in the RAAN distribution from 100 to 180° and also 200 to 360°, while for the selected TLE population this parameter is more or less equally distributed from 0 to 360°. These gaps are caused by the fact that we didn't survey continuously the entire stripe in RA due to the limited observation time at the ESASDT in specific months (see Fig. 10). For the inclination and eccentricity plotted in the middle figure we got distributions inside the selected TLE population (October 2013). It is obvious from the figure that some regions in inclination, as well as eccentricity, were not covered by our surveys. This was expected, because the population objects with eccentricities below 0.65 and with inclinations above 65° are objects with perigees situated above the northern hemisphere. In Fig. 2 these objects have the argument of perigee below 180°. Our observation strategy was not designed to cover this specific type of Molniya population. For perigee altitudes we obtained similar distribution as the selected TLE population. This can be seen in the lower figure. The catalogued UCTs cover perigee altitudes between 500 to 2,000 km which means that in most cases they are crossing the LEO region.

SURVEY EFFICIENCY

To investigate the detection efficiency of the Molniya survey, we simulated the observation campaign by using ESA's PROOF program and the TLE population. The goal was to investigate how efficient we were in detecting correlated targets (CT) during our campaign.

To simulate the observations we summarized all thirteen measurement nights and their OUs dedicated to the Molniya surveys. We used the same observation times and line of sights (LOS) (pointing directions) as they were used during the real observations, so we

reconstructed exactly the same observation parameters as they were used during the OGS observations. For every night we used the USSTRATCOM TLE catalogue of the given date as input for ESA's PROOF. To optimize the simulation processing time, we excluded all LEO objects (objects with semi-major axis < 8378.15 km) and all other objects with inclination less than 20°. These couldn't be observed under any circumstances from ESASDT's location and by using the given pointing directions. Finally, we investigated, which CTs should be detected by ESASDT during the given night and in a specific OU and we compared these results with the observed detections.

There were in total 57 objects with two and more detections during PROOF simulations. All of them were investigated and compared to the observations in order to investigate whether or not they have been tracked during the surveys. If not, an additional investigation was performed aiming to explain this discrepancy. From these 57 objects 25 (43.9 %) were detected by our automatic processing software. Further investigation showed that the majority of undetected CTs had an in-sufficient number of positions (less than three) per tracklet to be recognized by the software. This was caused either by situations when the objects had high angular velocities, or by objects crossing the FoV close to the FoV boundaries. For the Molniya objects, for which we optimized the pointing and blind tracking during the campaign, we detected 15 of 26 CTs which crossed the FoV in the PROOF simulation. This would mean that we achieved an average detection efficiency of 57.7 % for a reference subpopulation of Molniya objects, which crossed the FoV during surveys. By assuming that we detected 30 UCTs with the same detection efficiency, we estimate the number of UCTs which theoretically crossed our FoV during the surveys to be 52 UCTs.

On average there were 169 Molniya objects in the TLE population during the thirteen nights of observations. Of these a subset of 26 objects crossed the FoVs during the surveys. This would mean we achieved coverage of 15.4 % for the whole CT Molniya population. This estimate is fully consistent with the results obtained from the coverage simulation. Let's assume that the orbital distributions and detection efficiencies are identical for CT and UCT populations. Combining the total detection of UCTs (30) with the efficiency determined for CTs (57.7 %) and the CT population coverage determined from PROOF simulations (15.4 %), we can estimate the total number of UCT objects in Molniya type of orbit with magnitude brighter than ~19^{th} magnitude, to be 338 UCTs in total. Obviously, this result is just a raw estimate, as only a small fraction of the Molniya orbit region could be covered during the surveys.

In order to estimate the margin of error for the estimated total number of UCTs, we define the so-called sample portion to be $p = n/N$, where $n = 15$ is the number of CT detections and $N = 169$ is the total CT population. With confidence level of 95 % which corresponds to percentage confidence $z = 1.96$, we can calculate the margin of error e to be

$$e = z * \sqrt{\frac{p*(1-p)}{n}} = 1.96 * \sqrt{\frac{0.089*(1-0.089)}{15}} = 0.144 = 14.4\ \% \quad (1)$$

With this margin error the total size of UCT population would be 338 ± 48.7 objects for confidence level of 95 %. It has to be added that these numbers are valid only if the UCT and CT populations would be identical in sense of orbital distribution and survey detection efficiency.

SUMMARY

In this paper we introduced the highly eccentric and inclined population in Molniya types of orbit. The analysis of the TLE population (of January 2012, and January to August 2013) showed that there are about 170 known objects in the Molniya region and that this region is comparably sparsely populated. By simulating the evolution of orbital elements for the catalogued objects we showed that the distribution of the orbital elements of the current population should be similar to an assumed initial distribution.

A synthetic population of 900 objects was used to perform coverage simulations for possible survey strategies that we propose in this work. By using the ESASDT telescope, the entire scan of the Molniya region is ambitious due to the small FoV. We found that for a scenario that assumes three nights of observations each month for one year, a total of 16% of the Molniya population could be detected on at least one frame. This would already allow for a significant statistical analysis of the space debris population in the selected region.

During thirteen nights in 2013 we performed surveys, which were dedicated and optimized for the Molniya population. During these surveys we used the ESA Space Debris Telescope (ESASDT), which is part of the Optical Ground Station (OGS) situated in Tenerife, Canary Islands. We detected 15 correlated (CT) and 30 un-correlated Molniya targets (UCTs) when the correlation was done with ESA's DISCOS orbit catalogue. This means that we had twice the number of detections for UCTs than CTs. In order to ensure re-acquisition of these newly discovered objects two follow-up observations within the discovery night were acquired.

Out of all detected UCTs, 25 were chosen for additional follow-ups, which implies that these objects were added into the AIUB's internal catalogue and scheduled for further follow-up observations. For two newly discovered objects we determined an area-to-mass ratio (AMR) of 3.59 and 3.74 m^2/kg, which means that high area-to-mass ratio objects (HAMR) exists in Molniya-type orbits.

We analyzed the efficiency of the Molniya survey strategies through ESA's Program for Radar and Optical Observation Forecasting (PROOF) and available TLEs from DISCOS database. We estimated an efficiency of 57.7 % for Molniya CTs, for which the survey was optimized due to the blind tracking. The total coverage for CT population during performed surveys was estimated to be 15.4 %. In case that CT and UCT populations would be identical in sense of orbital distribution and detection efficiency, with 30 UCTs detected during our surveys and with the mentioned detection efficiency of 57.7 %, one can roughly estimate the number of objects which crossed our FoV during the surveys to be 52 UCTs. By applying the total coverage for CT population to UCT population we would get for the whole Molniya UCT population 338 ± 48.7 objects with confidence level of 95 %. These objects are in principle detectable by the ESASDT, which means objects with a limiting magnitude of about 19^{th} corresponding to a size of about 0.2 m in diameter for Lambertian sphere with a Bond albedo of 0.2.

It can be concluded that the observation strategy developed a by the Astronomical Institute University Bern (AIUB) in collaboration with the European Space Agency (ESA), is highly efficient in order to detect uncorrelated targets in Molniya type orbits. Our surveys and their results demonstrated that the Molniya region is much more densely populated than it is suggested in the publicly available TLE catalogue. Only about one third of the population observable by ESASDT telescope is actually catalogued today. Our limited sampling of orbital regimes requires to perform further Molniya survey in order to increase the level of

confidence about the knowledge of this newly discovered space debris population, including accessing the spatial distribution of objects, as well as their dynamical and physical characteristics. The goal is to provide sufficient observation data for the further improvement and validation of space debris environment models such as ESA MASTER model.

Acknowledgement: This work was performed under the ESA Contract 4000104923/11/D/JR.

REFERENCES:

Abercromby, K. J., Seitzer, P., Cowardin, H. et al., Survey and chase: A new method of observations for the Michigan Orbital DEbris Survey Telescope (MODEST), Acta Astronautica, Volume 65, Issues 1–2, July–August 2009, Pages 103-111, ISSN 0094-5765.

Beutler, G., "Methods of Celestial Mechanics", Springer Verlag, Heidelberg, 2005.

Flegel, S.K., Gelhaus, J. et al., Multi-layer insulation model for MASTER-2009, Acta Astronautica, Volume 69, Issues 11–12, December 2011, Pages 911-922, ISSN 0094-5765, http://dx.doi.org/10.1016/j.actaastro.2011.06.015.

Hernández, C., Pina Caballero, F., Sánchez Ortiz et al., DISCOS database and Web interface, In: Proceedings of the Third European Conference on Space Debris, 19 - 21 March 2001, Darmstadt, Germany. Ed.: Huguette Sawaya-Lacoste. ESA SP-473, Vol. 2, Noordwijk, Netherlands: ESA Publications Division, ISBN 92-9092-733-X, 2001, p. 803 – 807.

Krag, H., Bendisch, J. et al., Debris model validation and interpretation of debris measurements using ESA's proof tool, Acta Astronautica, Volume 48, Issue 5, 2001, Pages 373-383, ISSN 0094-5765

Krisko, P.H., Flegel, S. et al., ORDEM 3.0 and MASTER-2009 modeled debris population comparison, Acta Astronautica, Volume 113, August–September 2015, Pages 204-211, ISSN 0094-5765.

Molotov, I., Agapov, V. Titenko, V. et al., International scientific optical network for space debris research, Advances in Space Research, Volume 41, Issue 7, 2008, Pages 1022-1028, ISSN 0273-1177, http://dx.doi.org/10.1016/j.asr.2007.04.048.

Schildknecht, T., Musci, R., Ploner, M. et al., Optical observations of space debris in GEO and in highly-eccentric orbits. *Advances in Space Research* 34 (5), pp. 901-911, 2004.

Schildknecht, T., Musci, R., Flury, W. et al., Optical Observations of Space Debris in High-Altitude Orbits. *Proceedings of the 4th European Conference on Space Debris (ESA SP-587). 18-20 April 2005, ESA/ESOC, Darmstadt, Germany,* pp. 113-118, 2005.

Schildknecht, T., A. Vananti, J. Herzog et al, Optical Surveys for Space Debris in MEO. Proceedings of 9th US-Russian Space Surveillance Workshop, Listvyanka (Irkutsk), Russia, 2012.

Wiedemann, C., Flegel, S., Gelhaus, J. et al., The space debris environment model MASTER-2009, 28th International Symposium on Space Technology and Science (ISTS), 5-12 June 2011, Okinawa, paper 2011-r-22, 2011.

Xu, Y.-L., Horstman, M., Krisko, P. H. et al., Modeling of LEO orbital debris populations for ORDEM2008, Advances in Space Research, Volume 43, Issue 5, p. 769-782, 2009.

FIGURE CAPTIONS

Fig. 1 - Distribution of four orbital elements of the selected TLE population in January 2012.

Fig. 2 - Relation between orbital elements of the selected TLE population. The crosses indicate that these objects have an eccentricity less than 0.65 and the empty squares indicate that these objects have a perigee of less than 180°. The filled circles represent the rest of the Molniya population.

Fig. 3 - On the left, apparent passes in the topocentric right ascension and declination of the selected population seen from the OGS during one night in January 2012. On the right, topocentric angular velocities as a function of a topocentric declination seen from the OGS.

Fig. 4 - Evolution of orbital elements during 20 years for the selected TLE population assuming an *AMR* value of 0.009 kg/m^2 for atmospheric drag and radiation pressure. Objects with an eccentricity less than 0.65 are given in gray.

Fig. 5 - Distributions of four orbital elements of the selected TLE population in January 2012 (black) and after 20 years of prediction (gray). Compared are relative frequencies.

Fig. 6 - Relation between orbital elements of the synthetic population. The crosses indicate that these objects have an eccentricity less than 0.65 and the empty squares that these objects have a perigee of less than 180°. The filled circles represent the rest of the Molniya population.

Fig. 7 - Position of the observations fields in three simulated strategies.

Fig. 8 - Survey strategy with 3 fields per month displaced by 10° in right ascension.

Fig. 9 - Results of the coverage simulation with synthetic population after one year with 3 nights/fields of observations per month. Data for crossings (object which crossed the FoV) are plotted.

Fig. 10 - Thirteen surveyed fields (marked as black squares) during Molniya surveys performed within thirteen nights in 2013 with the ESASDT telescope. Fields were defined by geocentric right ascension and declination assuming object geocentric distance equals 41,000 km. Over the squares are listed numbers of UCTs and below numbers of CTs detected during given survey night.

Fig. 11 - Distribution of the magnitude of the discovered objects. To 10th of October 2013.

Fig. 12 - Variation of the magnitude of discovered object E13010B.

Fig. 13 - Estimated AMR values for objects with the observation arc length larger than 29 days. To 10th of October 2013.

Fig. 14 - Comparison between orbital elements of TLE population (reference epoch 20131010) and 24 UCTs catalogued during the Molniya surveys (reference epoch equals the date of discovery for given object). Plotted are RAAN vs argument of perigee (upper figure), inclination vs eccentricity (middle figure) and perigee vs argument of perigee (lower figure).

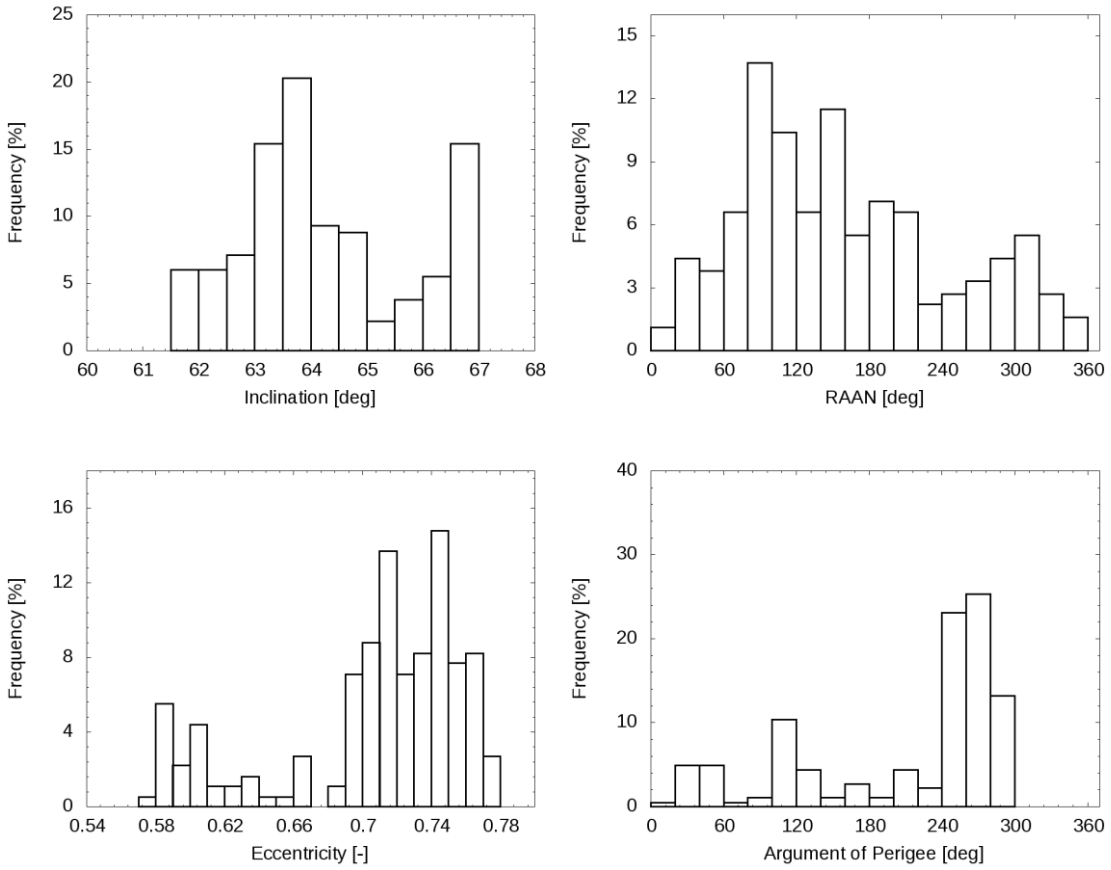

Fig. 1 - Distribution of four orbital elements of the selected TLE population in January 2012.

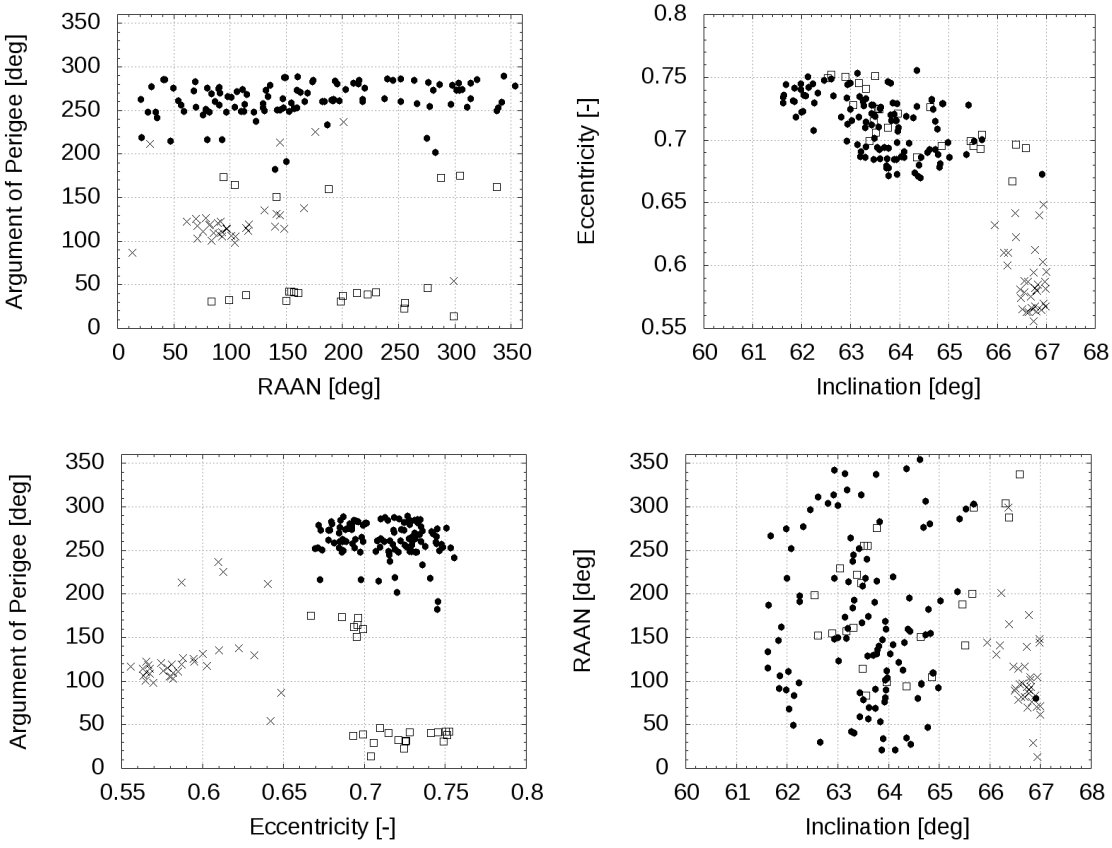

Fig. 2 - Relation between orbital elements of the selected TLE population. The crosses indicate that these objects have an eccentricity less than 0.65 and the empty squares indicate that these objects have a perigee of less than 180°. The filled circles represent the rest of the Molniya population.

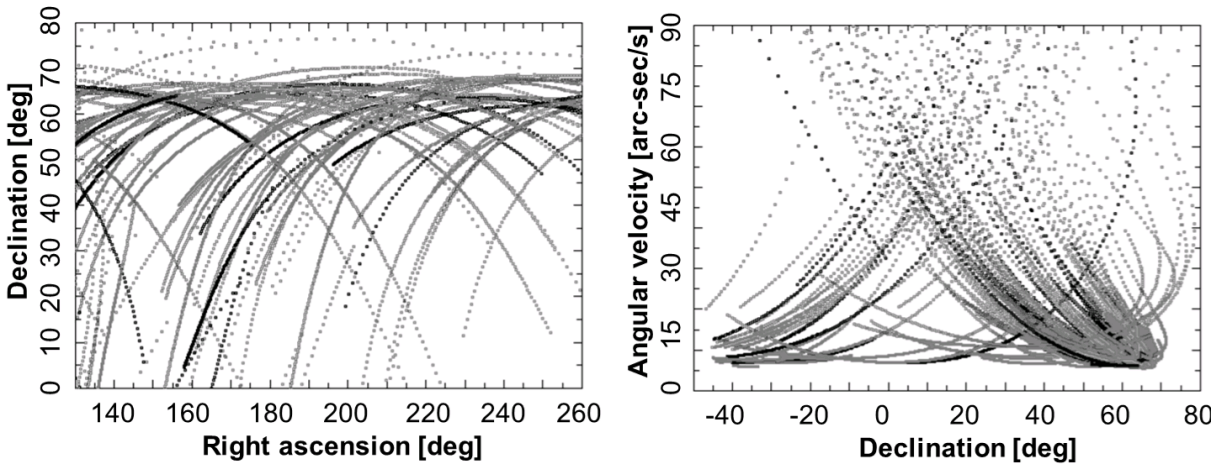

Fig. 3 - On the left, apparent passes of the selected population in the right ascension and declination seen from the OGS during one night in January 2012. On the right, topocentric angular velocities as a function of topocentric declination seen from the OGS.

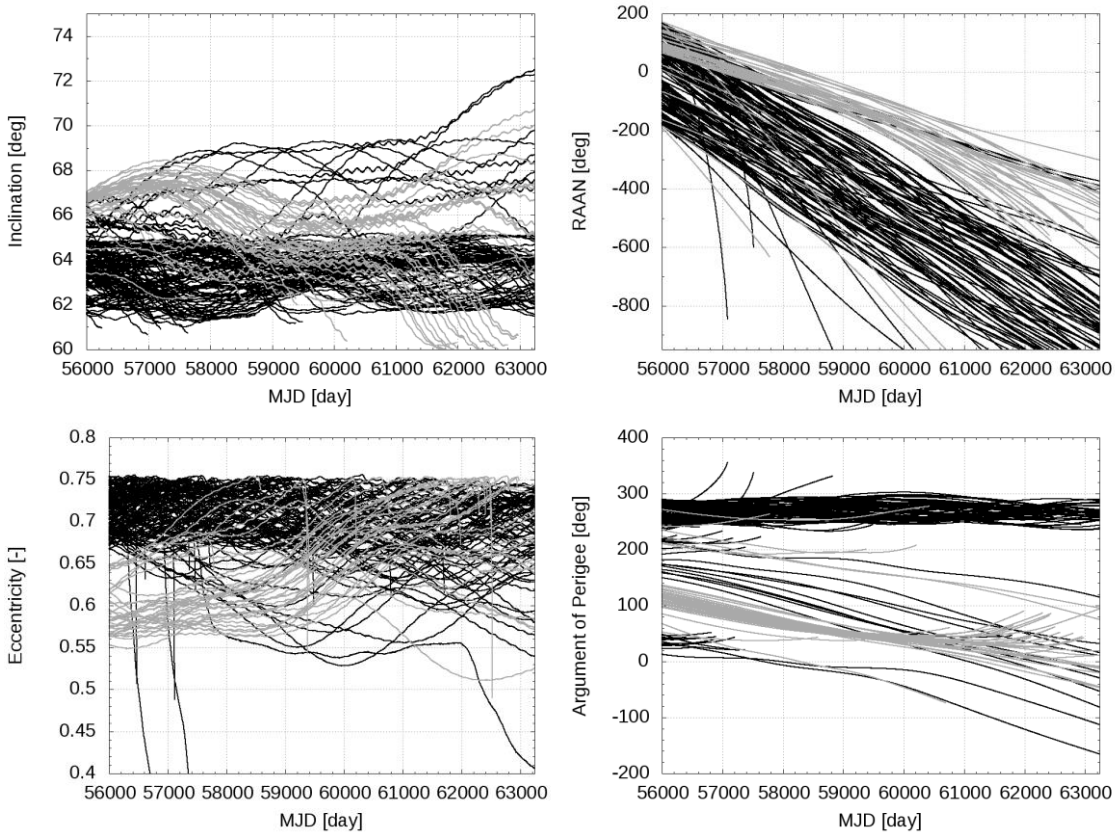

Fig. 4 - Evolution of orbital elements during 20 years for the selected TLE population assuming an *AMR* value of 0.009 kg/m^2 for atmospheric drag and radiation pressure. Objects with an eccentricity less than 0.65 are given in gray.

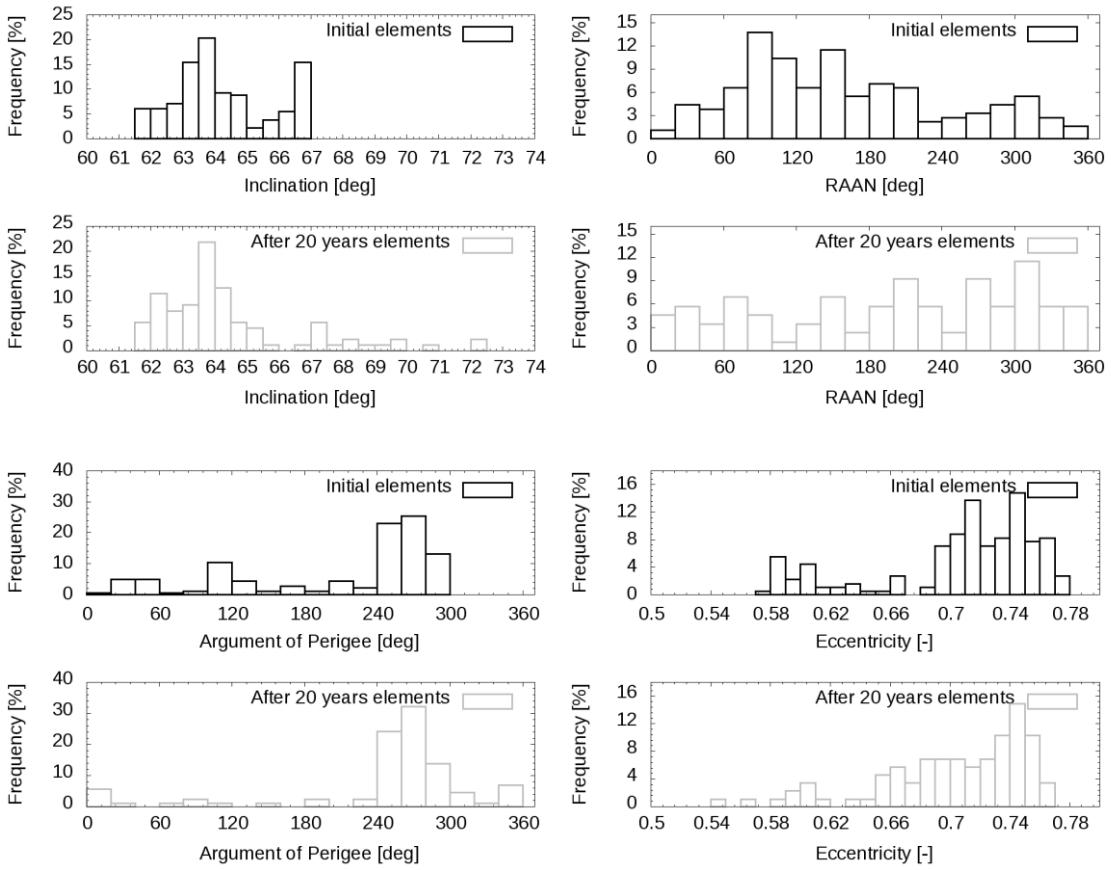

Fig. 5 - Distributions of four orbital elements of the selected TLE population in January 2012 (black) and after 20 years of prediction (gray).

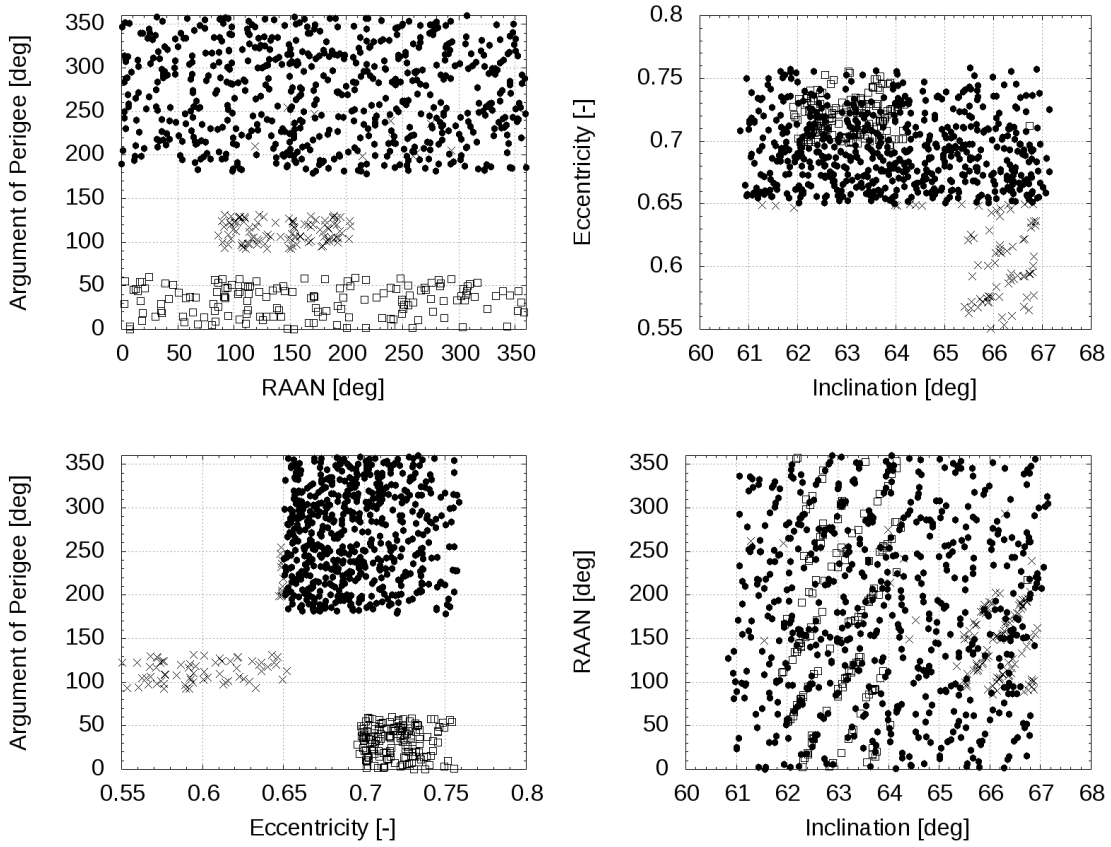

Fig. 6 - Relation between orbital elements of the synthetic population. The crosses indicate that these objects have an eccentricity less than 0.65 and the empty squares that these objects have a perigee of less than 180°. The filled circles represent the rest of the Molniya population.

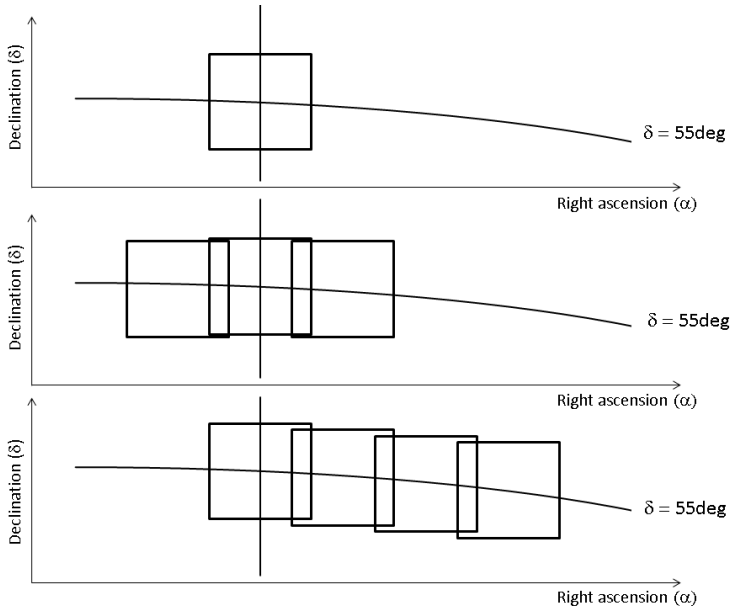

Fig. 7 - Position of the observations fields in three simulated strategies.

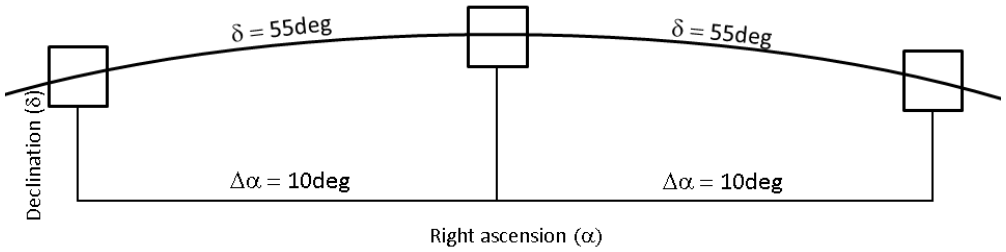

Fig. 8 - Survey strategy with 3 fields per month displaced by 10° in right ascension.

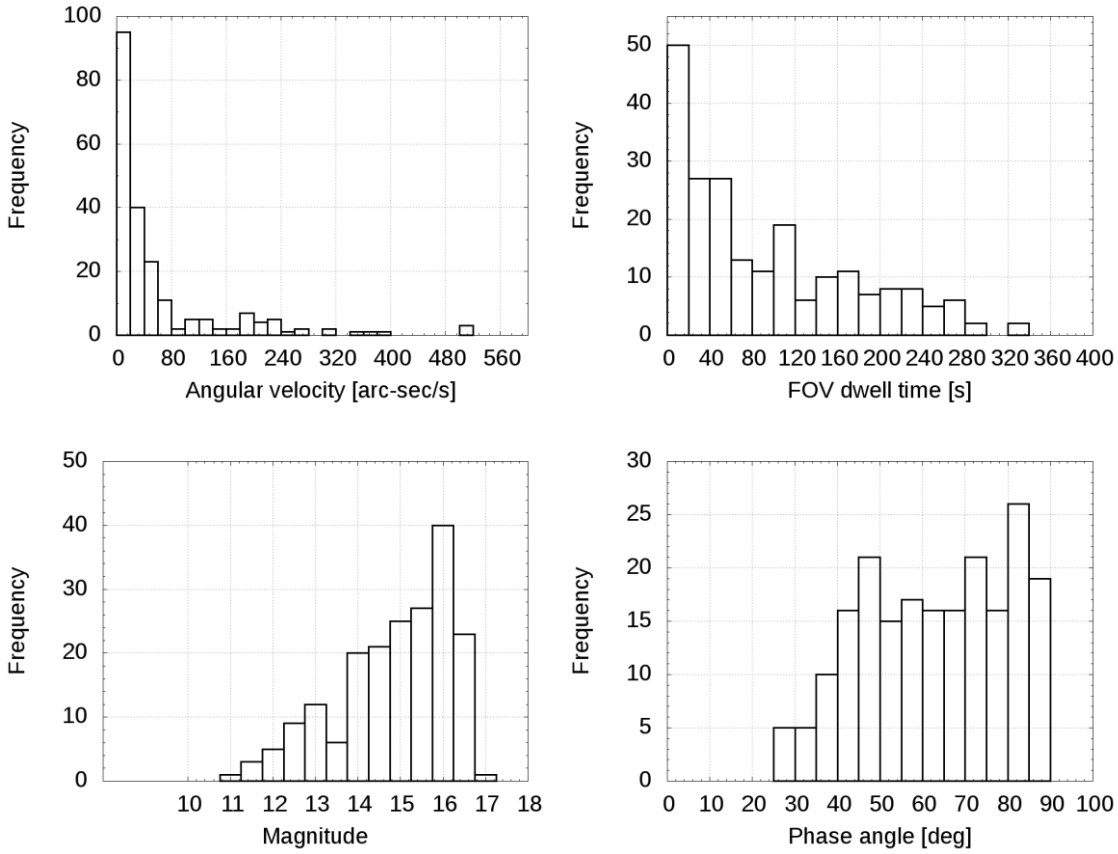

Fig. 9 - Results of the coverage simulation with a synthetic population after one year with 3 nights/fields of observations per month. Data for crossings (object which crossed the FoV) are plotted.

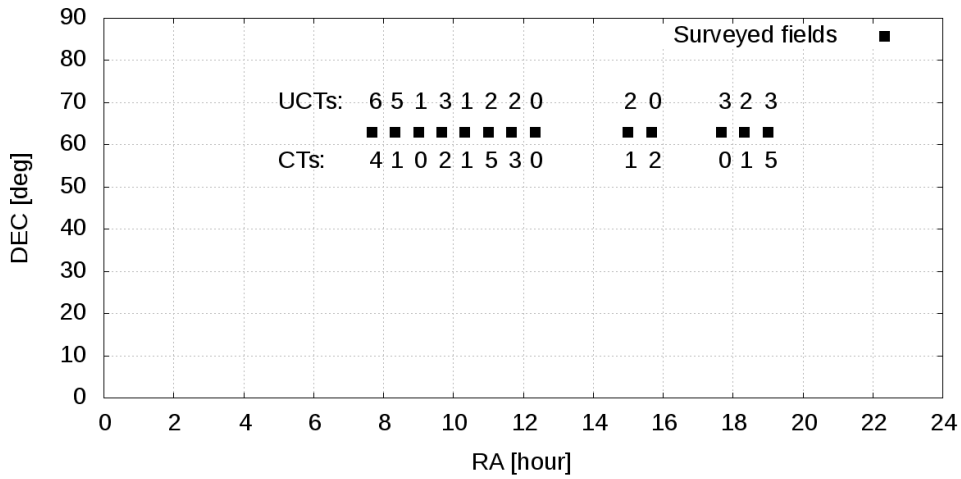

Fig. 10 - Thirteen surveyed fields (marked as black squares) during Molniya surveys performed within thirteen nights in 2013 with the ESASDT telescope. Fields were defined by geocentric right ascension and declination assuming object geocentric distance equals 41,000 km. Numbers above the squares indicate the numbers of UCTs and the ones below the squares the numbers of CTs detected for a given survey field.

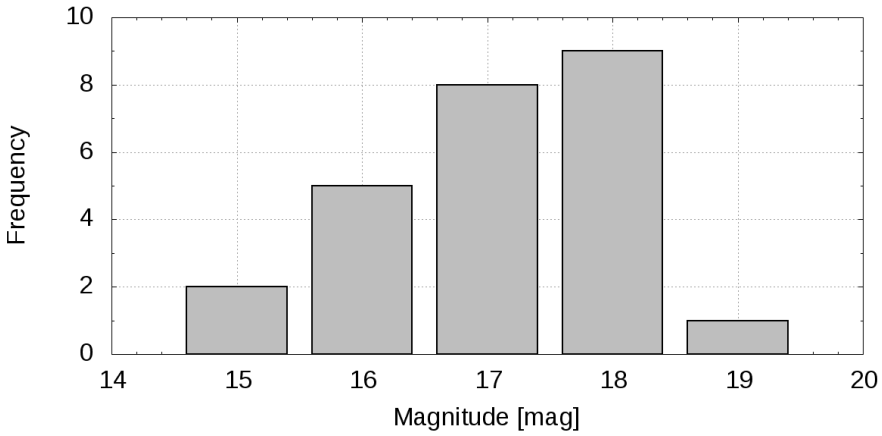

Fig. 11 - Distribution of the magnitudes of the discovered objects.

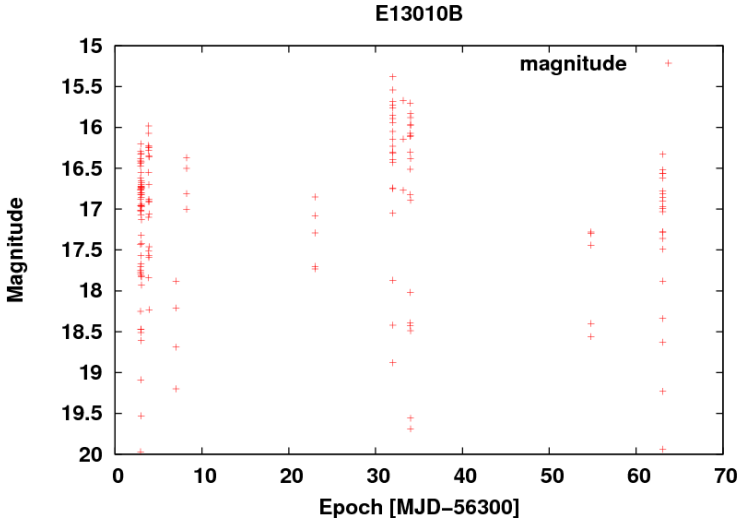

Fig. 12 - Variation of the magnitude of discovered object E13010B.

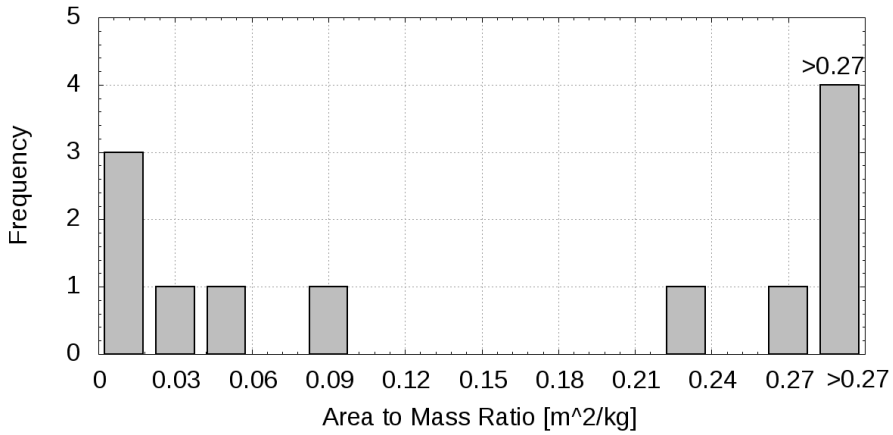

Fig. 13 - Estimated AMR values for objects with the observation arc length larger than 29 days. As of 10th of October 2013.

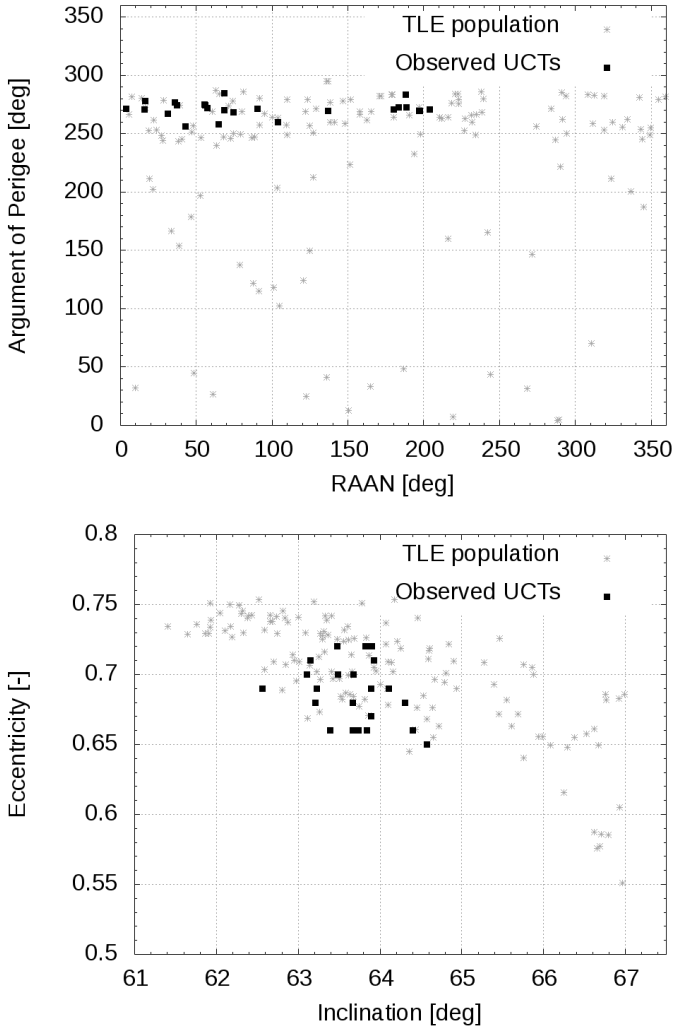

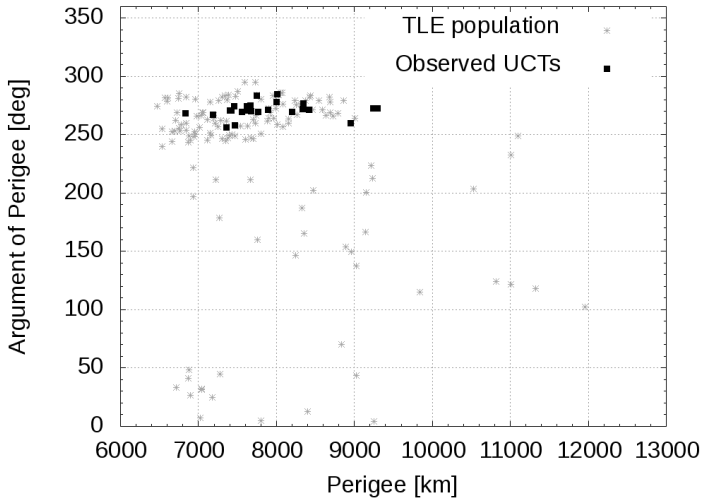

Fig. 14 - Comparison between orbital elements of TLE population (reference epoch 20131010) and 24 UCTs catalogued during the Molniya surveys (reference epoch equals the date of discovery for given object). The individual figures show the RAAN vs argument of perigee (upper figure), inclination vs eccentricity (middle figure) and perigee vs argument of perigee (lower figure).